AIP | Journal of Applied Physics

Effect of adsorbates on field-electron emission from ZnO nanoneedle arrays

H. Z. Zhang, R. M. Wang, and Y. W. Zhu

Citation: J. Appl. Phys. 96, 624 (2004); doi: 10.1063/1.1757653
View online: http://dx.doi.org/10.1063/1.1757653
View Table of Contents: http://jap.aip.org/resource/1/JAPIAU/v96/i1
Published by the AIP Publishing LLC.

Additional information on J. Appl. Phys.

Journal Homepage: http://jap.aip.org/
Journal Information: http://jap.aip.org/about/about_the_journal
Top downloads: http://jap.aip.org/features/most_downloaded
Information for Authors: http://jap.aip.org/authors

ADVERTISEMENT

Downloaded 08 Sep 2013 to 128.197.27.9. This article is copyrighted as indicated in the abstract. Reuse of AIP content is subject to the terms at: http://jap.aip.org/about/rights_and_permissions

HTML ABSTRACT + LINKS

Effect of adsorbates on field-electron emission from ZnO nanoneedle arrays

H. Z. Zhang and R. M. Wang[a)]
Electron Microscopy Laboratory and State Key Laboratory for Mesoscopic Physics, School of Physics, Peking University, Beijing 100871, People's Republic of China

Y. W. Zhu
Department of Physics, National University of Singapore, Singapore 117542, Singapore

(Received 12 December 2003; accepted 12 April 2004)

We studied the influence of adsorbates on field emission (FE) properties of well-aligned ZnO nanoneedle arrays with varying initial electric field, vacuum gap, and ambient pressure. The FE current exhibits hysteresis upon a loop of applied voltage. On applying an initial electric field of 3.85×10^{6} V/m, the turn-on voltage increases ~50%, Fowler-Nordheim plots show better linearity, as well as the hysteretic behavior can be annihilated. It is found that the FE current depends on the vacuum gap and the ambient pressure. The FE current increased sensitively with increasing the ambient pressure P when $P<\sim7\times10^{-5}$ Pa, and it saturates in the pressure range of $7\times10^{-5}-3\times10^{-4}$ Pa above which the FE current drops. The phenomena can be explained by the adsorbate effects. The adsorbate states modify the effective work function of the samples, and two emission regimes, adsorption-controlled and desorption-controlled processes, were proposed. Our results are useful for practical applications as the $I-V$ characteristics can be affected by environmental parameters, especially the ambient pressure. © *2004 American Institute of Physics.* [DOI: 10.1063/1.1757653]

I. INTRODUCTION

Field emission (FE) concerning electrons tunneling to the vacuum through a field-modified surface barrier has been extensively studied. The Fowler-Nordheim (FN) theory of FE has been proved to be quite successful in describing electron emission from metallic surfaces.[1] However, to analyze a FE device is often much complicated. Moreover, the applications of the FE devices, e.g., flat panel display (FPD), require emitters exhibiting low turn-on voltage, large FE current density, reproducibility, stability, and good retention and fatigue-resisting properties[2,3] among which some of them cannot be explained solely on the FN theory. For example, the shape of the emitter affects its FE properties significantly.[4–6] Emitters with large aspect ratios, such as carbon nanotubes (CNTs), show much better FE properties than the flat samples due to the enhancement of the local field.[7] The prototype of CNTs-based FPD has been thus fabricated.[8] Recently, low-dimensional oxides have stimulated much research interests for their potential applications in FE devices.[9,10] Compared with CNTs, oxide emitters are more stable in harsh environment and controllable in electrical properties.[11–13] As a wide band-gap semiconductor, ZnO exhibits many fascinating electrical and optical properties. It can be *n*-type doped with nitrogen or simply through oxygen vacancies to reach a high carrier (electron) density, which can support a large electron disbursement in FE operation, i.e., a large emission current.[14] Furthermore, ZnO nanoneedle arrays have been successfully fabricated recently.[15,16] The high aspect ratio of the individual nanoneedle and the good alignment between the nanoneedles can dramatically enhance the local electrical field and thus increase the emission current. Up to now, the FE properties of ZnO nanoneedle arrays, nanorod arrays, and single nanowire have been explored.[16–18] The nanoscaled ZnO emitters may have low turn-on voltage and high current density, which are comparable to those of CNTs.[16] However, the physics of the high FE performance of the ZnO nanostructures still remains unclear. Dong *et al.* proposed that the high FE originated from adsorbates and the emission followed FN relation in the case of single ZnO nanowire emitter,[18] whereas, in general, the effect of adsorbates on the FE properties are also ambiguous. For the CNT emitters, different experimental results and theoretical models concerning adsorptions including the space charge[19] and cathode adsorption models[20] have been proposed. It is hence worthy to investigate the adsorption-induced phenomena for ZnO emitters in the viewpoints of both fundamental physics and advanced technology. In this communication, we will discuss the effect of cathode adsorbates on the emission properties of ZnO nanoneedle arrays.

II. EXPERIMENTS

The ZnO nanoneedle arrays were synthesized through a selenium-controlled vapor phase chemical reaction. The details of the growth were described in our previous paper.[16] In this work, the morphologies and microstructures of the ZnO nanoneedle arrays were characterized using a field emission Strata DB235-FIB (FEI company, USA) working at scanning

[a)]Author to whom correspondence should be addressed; present address: National Center for Electron Microscopy, Lawrence Berkeley National Laboratory, University of California, CA 94720; electronic mail: rmwang@pku.edu.cn

 © 2004 American Institute of Physics

Downloaded 08 Sep 2013 to 128.197.27.9. This article is copyrighted as indicated in the abstract. Reuse of AIP content is subject to the terms at: http://jap.aip.org/about/rights_and_permissions

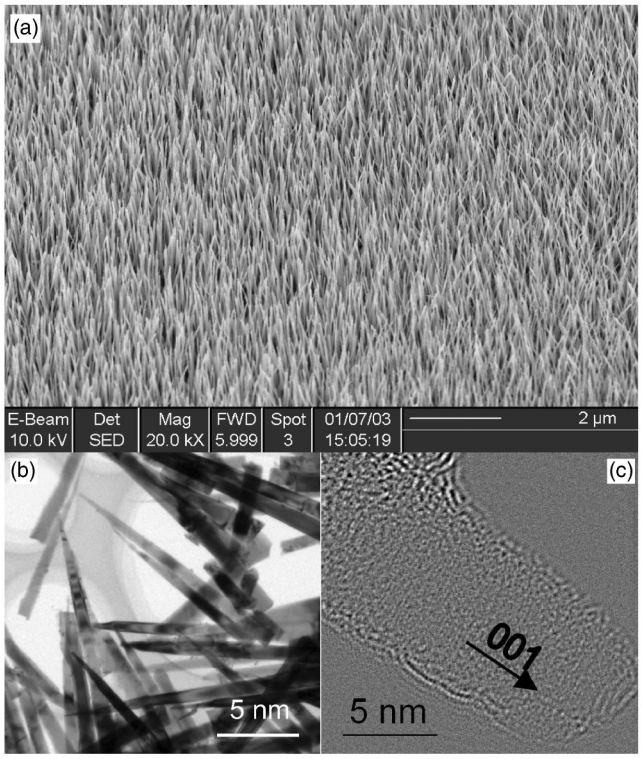

FIG. 1. (a) SEM image showing the general morphology of the well-aligned ZnO nanoneedle arrays grown on Si substrate. (b) TEM image of the ZnO nanoneedles. (c) HREM image showing the tiny tip of several nanometers of single nanoneedle.

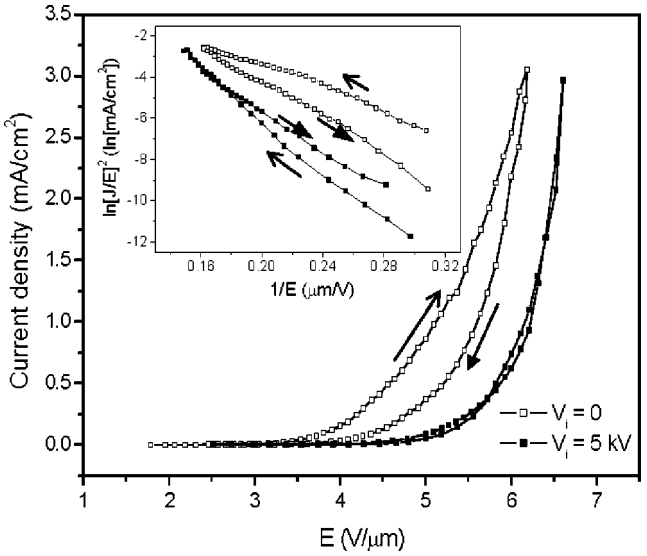

FIG. 2. Field emission $J-E$ curves with ($V_i=0$) and without ($V_i=5$ kV) the initial high-voltage pulse. The hysteretic window is largely depressed by applying the initial pulse. The inset shows the initial pulse makes the emission of the forward sweep closer to the FN behavior.

electron microscope (SEM) mode and a Tecnai F30 Transmission Electron Microscopy (TEM, FEI company, USA) with field-emission gun and accelerating voltage of 300 kV. The field-emission properties of the arrays were measured by using a two-parallel-plate configuration in an ultrahigh vacuum (UHV) chamber with the lowest pressure $\sim 3\times 10^{-7}$ Pa. The sample was adhered to one of the two stainless-steel plates as a cathode, and the other one was put parallel to the cathode and biased as anode. The distance between the two poles, the vacuum gap D, was adjusted by a fine micrometer with precision up to 5 μm. The emission current was measured using a Keithly 485 picoammeter. In order to remove contaminants from the sample, a high-voltage negative bias of 5 kV was applied to the tips whenever it was necessary before a measurement. The effect of the electric field was studied by conducting the similar measurement only without applying the initial high voltage. The influence of the adsorbates on FE properties of our samples was further elucidated by varying the vacuum gap D. We also investigated the effect of the ambient pressure, which was conducted by shutting down the ionic pump and recording the pressure versus the emission current under a constant applied voltage.

III. RESULTS AND DISCUSSIONS

A typical SEM image of the as-grown ZnO nanoneedle arrays was shown in Fig. 1(a). The substrate is covered uniformly by nanoneedle arrays with a high coverage. The nanoneedles with very sharp tips and stem diameters less than 100 nm are well aligned. The lengths of the nanoneedles usually exceed 3 μm. Figure 1(b) is the TEM image of the ZnO nanoneedles showing the sharp morphologies of the ZnO nanoneedle tips. High-resolution TEM (HRTEM) image shown in Fig. 1(c) reveals that the lateral dimension of the nanoneedle tip is only about 7 nm with the growth direction of [0001]. Other characterization methodologies demonstrated that the samples are well-crystallized ZnO nanoneedle arrays.[16]

To study the effect of the adsorption, we first compared the dependence of emission current density (J) on apparent field (E), which is defined as the applied voltage divided by the vacuum gap, with and without applying the initial voltage. In both cases, the vacuum gap was fixed at 1300 μm with chamber pressure $\sim 3\times 10^{-7}$ Pa. We emphasize that the apparent filed is not necessarily equal to the field actually exerting on the tips, since there are multiple tips with different heights and variations in density which makes it impossible to assume the shielding factors and to obtain the actual field adjacent to the tips. However, using the apparent field is convenient to elucidate the problem, since the vacuum gap is fixed for both cases. For the measurement using the initial electric field, a 5 kV negative bias with electric field of 3.85×10^{6} V/m was first applied for 5 min. After we turned off the high voltage, the emission current density J was then immediately recorded as a function of the apparent field. The applied voltages were first increased from 1 kV to 4 kV (forward branch) and then returned back to 1 kV (backward branch) with a step of 30 V at a rate of 1 step/min. Afterwards, before our conducting next measurement, the electric field was turned off and the sample was kept in the chamber with the high vacuum for 24 h to get rid of the possible influences resulting from the previous measurement. Successive comparative measurement was then conducted only without applying the initial voltage. The results are shown in Fig. 2, where the open-squared and solid-squared symbols

Downloaded 08 Sep 2013 to 128.197.27.9. This article is copyrighted as indicated in the abstract. Reuse of AIP content is subject to the terms at: http://jap.aip.org/about/rights_and_permissions

stand for the measurements without and with the initial voltage, respectively (Lines in Fig. 2 are only for reference). The open arrow ("↑") represents the forward branch while the closed one ("↑") represents the backward branch. Two differences can be apparently distinguished from the two curves: (1) For a given apparent electric field E, the emission current density J is smaller, and hence the turn-on field is larger when applying the initial electric field (~ 3 V/μm and ~ 4.5 V/μm corresponds to without and with the initial electric field, respectively). (2) Obvious hysteretic behavior is observed in the measurement without applying the initial electric field. The values of J of the backward branch (BB) are up to 50% smaller than those of the forward one. Such hysteretic behavior can be depressed and finally annihilated by applying the initial electric field $\sim 3.85\times 10^6$ V/m (as shown in Fig. 2). Such phenomena can always be observed in all our ZnO samples and for each sample the result is reproducible. From the above results, we can assign both the hysteresis and its depression to the intrinsic emission properties of the samples.

To reveal the physical nature of the phenomena, the FN plots of the forward branch (FB) and backward branch (BB) of the two measurements are depicted as inset in Fig. 2. The FN plots demonstrate the effect of the initial electric field as follows. First, the linearity of the FB versus that of BB depends on the initial electric field. Without applying the initial field, the linearity of the FB is worse than that of the BB, while the linearity of the FB is better than that of the BB in the case of applying the initial electric field of 3.85×10^6 V/m. Second, the FN slopes during decreasing the electric field are found to be almost the same for the measurements. Third, the relationships between the FN slopes of the BBs and the FBs are found to be related to the applied initial electric field as well. Without the initial electric field, the FN slope of the BB is larger than that of the FB. In the contrary, the FN slope of the BB is smaller than that of the FB in the case of applying the initial electric field. According to the FN theory, the slope of the FN curve, S, can be written as, $S=-2.83\times 10^7\phi^{3/2}/\beta$, where ϕ is the work function of the emitter and β is the field enhancement factor. It is clear that the slope of the FN curve is a function of the work function ϕ and the field enhancement factor β. Any change in the two quantities can affect the slope. It is well known that β is strongly dependent on the geometric configuration of the samples.[4–6] For a single sample, the variation of β due to the change in its geometric configuration means that such variation would be irreversible and a serious damage to the morphology of the sample should be observed. In our case, however, neither of these is true. While the emitters higher and sharper than the surrounding ones can be dulled back and β can thus be changed, such effect is not dominant for our sample. In spite of some announcements that β can be adjusted by the space charge and other nongeometric factors:[7,21,22] in our cases, we can safely assume that β does not change too much for the measurements because of both the similar high aspect ratios of the ZnO nanoneedle tips and the ultrahigh vacuum. Therefore, the variation of the slopes of the FN curves can be mainly attributed to the modification of the work function. The work functions are then calculated to be about 3.6 eV (4.4 eV) for the FB (BB) without the initial electric field and 5.4 eV (4.8 eV) for those with the initial electric field of 3.85×10^6 V/m, respectively. During the calculation, we assume the work function of the FB with the initial voltage is the same as that of the ZnO (5.4 eV),[16] which is reasonable because the absorbates can be desorbed by applying the high voltage. It is worthy noticing that the work functions calculated for the other branches are smaller than that of bulk ZnO, which is a typical phenomenon of the cathode absorbates by inducing a number of surface states. The formation of the surface states can thus dramatically lower the effective work function.[23–25] As to the variation of the work functions for the forward and backward branches, we believe that the adsorbates were desorbed under the high voltage at the last stage of the forward branch in the case without using the initial voltage, while the adsorption rate was larger than the desorption rate at the process of backward branch as applying the initial electric field. The above discussion is self-consistent, however, the effect of the adsorbates on the FE properties has to be verified by other experiments.

To further explore the effect of the adsorbates, we measured the emission current and the applied voltage characteristics at different vacuum gaps (D).[26,27] Each measurement was conducted at intervals of 24 h and a bake-out was applied before each measurement to guarantee the same initial experimental conditions for these measurements except the D value. The apparent electric field between the cathode and the anode is $E=V/D$. Figure 3(a) shows the J-E curves under different anode-cathode distances. From Fig. 3(a) we can see that under the same electric field the larger the D, the smaller the emission current. Figure 3(b) shows the FN plots with different D values. In low-electric-field region, the emission demonstrates linear behavior in the FN plot, while the curves deviate from linear at high-field regime as divided by a dashed line in Fig. 3(b). We took the transition points, from which the FN plot deviate from linear and then calculated the electrical power density, i.e., $P_s=jU=jEd$. The electrical power densities are calculated to be 632 mW/cm^2, 622 mW/cm^2, and 657 mW/cm^2 corresponding to 520 μm, 560 μm, and 610 μm, respectively. At the transition points, the electrical powers for the three distances have similar values, which suggests the existence of a characteristic quantity related to the termination of FN behavior. The quantity can be derived by considering the desorption process. It is the emission current that provides the energy to remove the cathode adsorbates and the desorption process can be simply expressed as

$$\frac{dn}{dt}=-An\exp\left(-\frac{w_d}{E_k}\right), \tag{1}$$

where n is the density of the cathode surface adsorbates, w_d is the absorption energy of the adsorbates on the cathode surface, and E_k is the kinetic energy of the adsorbates. The adsorbates are directly heated by the emission current, hence, E_k is proportional to P_s. Therefore, it is reasonable to say that the quantity we defined above is w_d. Above-mentioned analysis naturally categorizes the whole emission curve into adsorbates-controlled and desorption-controlled regimes. In

Downloaded 08 Sep 2013 to 128.197.27.9. This article is copyrighted as indicated in the abstract. Reuse of AIP content is subject to the terms at: http://jap.aip.org/about/rights_and_permissions

the adsorbates-controlled regime the emission follows the FN mechanism, while it deviates from linearity when the desorption process is significant. The influence of the cathode-anode distance can also be understood in the same absorption frame. To explain it, we first calculate the impingement rate of the gas-phase molecules on the cathode surface, because it determinates the absorption rate directly. The mean free path of the molecules is given by $\bar{\lambda} = kT/(\sqrt{2}\pi d^2 p)$. The typical pressure in our experiment is about 10^{-7} Pa, so $\bar{\lambda} \approx 10^4$ m, which is much greater than the cathode-anode distance. Hence, we can ignore the contributions from the molecules between the electrodes and the ambient can be treated as ideal gas in equilibrium state. A spherical coordinate is used because it is convenient to handle the problem, as depicted in Fig. 4. The number of the impinging molecules on the cathode surface per unit area per unit time is given by

$$\begin{aligned}\Gamma_0 &= \int\int\int \nu n f(\bar{\nu}) \cos\theta d\bar{\nu} \\ &= n\int_0^{2\pi} d\varphi \int_\alpha^{\pi/2} \cos\theta \sin\theta d\theta \int_0^\infty \nu \left(\frac{m}{2\pi kT}\right)^{3/2} \\ &\quad \times e^{-(m\nu^2/2kT)} \nu^2 d\nu \\ &= \frac{p\cos^2\alpha}{\sqrt{2\pi mkT}}. \end{aligned} \tag{2}$$

Because the anode area is much larger than the cathode area, we can simply write the total impingement rate as the cathode area (S) times Γ_0:

$$\Gamma = S\Gamma_0 = \frac{pS\cos^2\alpha}{\sqrt{2\pi mkT}} = \frac{pS}{\sqrt{2\pi mkT}} \frac{D^2}{D^2+b^2} \propto D^2, \tag{3}$$

where b is the radius of the anode and the last step is under an approximation of $b \gg D$. According to Eq. (3), the absorption rate is proportional to D^2, which indicates the larger the distance, the more the adsorbates on the cathode surface in the adsorbates controlled regime. The above analysis suggests that the adsorbates can lower the effective work function. However, if the coverage of the adsorbates is too high to impede the emission from the ZnO emitters, the emission centers directly originate from the adsorbates, which can lower the emission quality due to either the low electron density of the adsorbates or the induced space charge region. This could be the reason for the distance effects, i.e., the larger the distance, the smaller the emission current under the same applied field. Here, we point out that the process can also result in the current saturation, see below and Ref. 28.

We also measured the emission current varying with the ambient pressure to clarify our models. The chamber pressure was changed from 3×10^{-7} Pa to 4×10^{-4} Pa continuously under the applied voltage and a constant cathode-anode distance. The result is shown in Fig. 5. It can be seen that the field-emission current is significantly enhanced when the pressure decreases from 3×10^{-7} Pa to 7×10^{-5} Pa. It is because the decreasing of gas pressure leads to the increase of gas molecule concentration, then a number of adsorbates

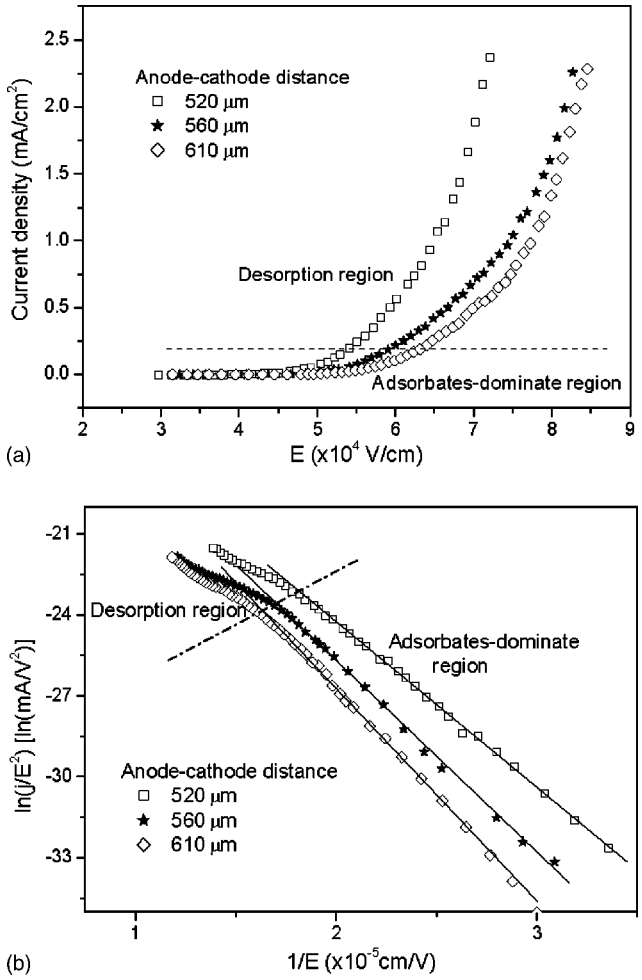

FIG. 3. (a) Field emission $J-E$ curves from the ZnO nanoneedle arrays at different anode-cathode distances: $d_1 = 520\ \mu$m, $d_2 = 560\ \mu$m, and $d_3 = 610\ \mu$m. The inset depicts the FN plot, which indicates in the low electronic field satisfying the FN mechanism by showing linear dependence while in the high electronic field deviating from the FN mechanism due to the desorption effects.

adhere to the emitter nanoneedles [see Eq. (3), $\Gamma \propto p$], so the adsorbates can lower the work function and make the emission current significantly enhanced. We also observed a saturation region as the pressure further decreased. The saturation current possibly results from the balance between the adsorption and desorption processes, while the coverage of adsorbates on the cathode surface still increases. As the pres-

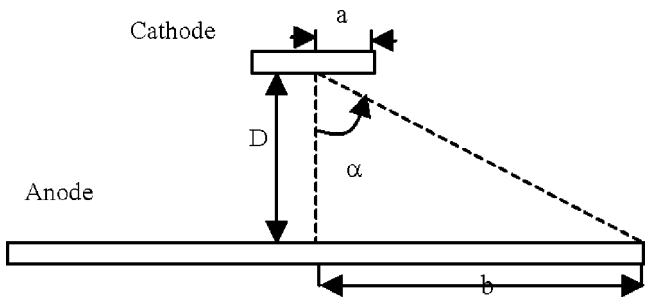

FIG. 4. Spherical coordinates sketch map of the anode-cathode configuration.

Downloaded 08 Sep 2013 to 128.197.27.9. This article is copyrighted as indicated in the abstract. Reuse of AIP content is subject to the terms at: http://jap.aip.org/about/rights_and_permissions

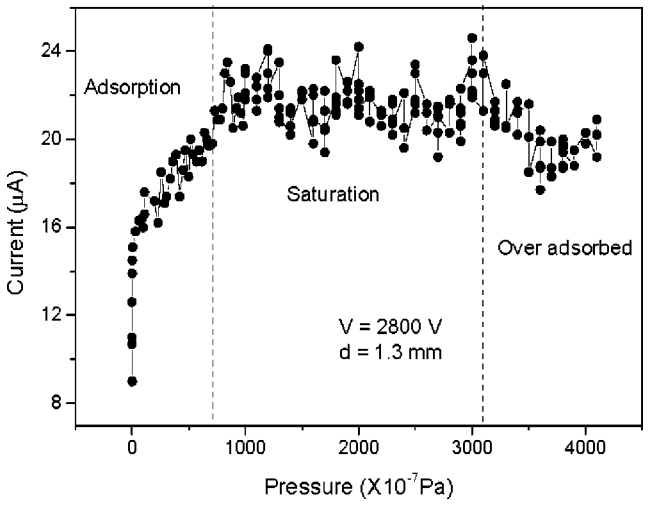

FIG. 5. Characteristic of the emission current via change of the vacuum pressure.

sure is larger than 3.1×10^{-4} Pa, the emission current starts dropping, which can be attributed to the over-adsorption effect as discussed above.

IV. CONCLUSIONS

In conclusion, field emission of ZnO nanoneedle arrays consists of the emission of adsorbate states on ZnO nanoneedles. The adsorbate states strongly enhance the emission efficiency, which can be attributed to the modification of the effective work function of the samples by the adsorbates. These results were strongly supported by a series of experiments under different initial voltage pulses, different vacuum gaps, as well as different vacuum pressures, respectively. Our results should be valuable to technical application because the design of FPD must consider the practical conditions of the emitters.

ACKNOWLEDGMENTS

This project is financially supported by National 973 Project (Grant No. 2002CB613505, MOST), the Scientific Research Foundation for the Returned Overseas Chinese Scholars (Grant No. EJ20030038), State Education Ministry, and the 31st Postdoc Research Foundation. R. M. Wang acknowledges support from the Berkeley Scholar Program.

[1] A. Modinos, Solid-State Electron. **45**, 809 (2001).
[2] K. Okano, S. Koizumi, S. P. Silva, and G. A. J. Amaratunga, Nature (London) **381**, 140 (1996).
[3] I. Musa, D. A. I. Munindrasdasa, G. A. J. Amaratunga, Nature (London) **395**, 362 (1998).
[4] K. Yuasa, A. Shimoi, I. Ohba, and C. Oshima, Surf. Sci. **520**, 18 (2002).
[5] R. G. Forbes and K. L. Jensen, Ultramicroscopy **89**, 17 (2001).
[6] R. B. Marcus, T. S. Ravi, T. Gmitter, H. H. Busta, J. T. Niccum, and K. K. Chin, IEEE Trans. Electron Devices **38**, 2289 (1991).
[7] C. Adessi and M. Devel, Phys. Rev. B **65**, 075418 (2002).
[8] D. Chung *et al.* Appl. Phys. Lett. **80**, 4045 (2002).
[9] C. J. Lee, T. J. Lee, S. C. Lyu, Y. Zhang, H. Ruh, and H. J. Lee, Appl. Phys. Lett. **81**, 3648 (2002).
[10] B. R. Chalamala, R. H. Reuss, K. A. Dean, E. Sosa, and D. E. Golden, J. Appl. Phys. **91**, 6141 (2002).
[11] K. A. Dean and B. R. Chalamala, Appl. Phys. Lett. **75**, 3017 (1999).
[12] J. M. Bonard and C. Klinke, Phys. Rev. B **67**, 115406 (2003).
[13] D. Kim, H. Yang, H. Kang, and H. Lee, Chem. Phys. Lett. **368**, 439 (2003).
[14] M. S. Chung, B. Yoon, J. M. Park, and K. Ha, Appl. Surf. Sci. **146**, 138 (1999).
[15] J. Wu and S. Liu, Adv. Mater. **14**, 215 (2002).
[16] Y. W. Zhu *et al.* Appl. Phys. Lett. **83**, 144 (2003).
[17] C. J. Lee, T. J. Lee, S. C. Lyu, Y. Zhang, H. Ruh, and H. J. Lee, Appl. Phys. Lett. **81**, 3648 (2002).
[18] L. Dong, J. Jiao, D. W. Tuggle, J. M. Petty, S. A. Elliff, and M. Coulter, Appl. Phys. Lett. **82**, 1096 (2003).
[19] N. S. Xu, Y. Chen, S. Z. Deng, J. Chen, X. C. Ma, and E. G. Wang, J. Phys. D **34**, 1597 (2001).
[20] A. Maiti, J. Andzelm, N. Tanpipant, and P. V. Allmen, Phys. Rev. Lett. **87**, 155502 (2001).
[21] G. L. Bilbro and R. J. Nemanich, Appl. Phys. Lett. **76**, 891 (2000).
[22] J. Chen, S. Z. Deng, J. C. She, N. S. Xu, W. Zhang, X. Wen, and S. Yang, J. Appl. Phys. **93**, 1774 (2003).
[23] M. Grujicic, G. Cao, and B. Gersten, Appl. Surf. Sci. **206**, 167 (2003).
[24] S. Han and J. Ihm, Phys. Rev. B **61**, 9986 (2000).
[25] R. Collazo, R. Schlesser, and Z. Sitar, Diamond Relat. Mater. **11**, 769 (2002).
[26] P. G. Collins and A. Zettl, Phys. Rev. B **55**, 9391 (1997).
[27] D. Y. Zhong, G. Y. Zhang, S. Liu, T. Sakurai, and E. G. Wang, Appl. Phys. Lett. **80**, 506 (2002).
[28] K. A. Dean and B. R. Chalamala, Appl. Phys. Lett. **76**, 375 (2000).

Downloaded 08 Sep 2013 to 128.197.27.9. This article is copyrighted as indicated in the abstract. Reuse of AIP content is subject to the terms at: http://jap.aip.org/about/rights_and_permissions